HHS Public Access

Author manuscript

*J Biomed Mater Res A*. Author manuscript; available in PMC 2022 April 28.

Published in final edited form as:

*J Biomed Mater Res A*. 2021 August ; 109(8): 1393–1405. doi:10.1002/jbm.a.37131.

# Development of a Dinutuximab Delivery System Using Silk Foams for GD2 Targeted Neuroblastoma Cell Death

**Kimberly J. Ornell, ME**[1], **Bill Chiu, MD**[2,3], **Jeannine M. Coburn, PhD**[1,*]

[1]Department of Biomedical Engineering, Worcester Polytechnic Institute, Worcester, MA;

[2]Department of Surgery, Division of Pediatric Surgery, University of Illinois at Chicago, Chicago, IL;

[3]Department of Surgery, Division of Pediatric Surgery, Stanford University, Stanford, CA

## Abstract

Neuroblastoma is the most common extracranial solid tumor of childhood and is associated with poor survival in high risk patients. Recently, dinutuximab (DNX) has emerged as an effective immunotherapy to treat patients with high risk neuroblastoma. DNX works through the induction of cell lysis via complement-dependent cytotoxicity (CDC) or antibody dependent cellular cytotoxicity (ADCC). However, one third of patients who undergo DNX treatment exhibit tumor relapse and the therapy is dose limited by side effects such as severe pain. To overcome delivery challenges of DNX, including large size and dose limiting side effects, we fabricated a delivery system capable of sustained local delivery of bioactive DNX utilizing silk fibroin. We evaluated the impact of silk properties (MW, crystallinity, and concentration) on release properties and confirmed the bioactivity of the release product. Additionally, we observed that the effectiveness of CDC induction by DNX could be correlated to the GD2 expression level of the target cells, with both the intravenous DNX formulation and the released DNX. Collectively, this data highlights a strategy to overcome delivery challenges and potentially improve therapeutic efficacy in cells expressing heterogenous levels of GD2.

### Keywords

Neuroblastoma; GD2; silk fibroin; sustained release; dinutuximab

## Introduction

Neuroblastoma is the most common extracranial solid tumor of childhood, accounting for 6% of all childhood cancers. Approximately 90% of patients are younger than 5 years of age at diagnosis, and approximately 55% of patients have metastasis at the time of diagnosis.[1] Treatment for neuroblastoma is multimodal and typically consists of surgical resection, radiation, and chemotherapy.[2] Recently, immunotherapy has emerged as a promising method of treatment for advanced stage neuroblastoma.[2] The primary immunotherapeutic target

[*]Corresponding Author: Dr. Jeannine M. Coburn, Assistant Professor of Biomedical Engineering, Worcester Polytechnic Institute, 60 Prescott Street, Rm 4035, Worcester, Massachusetts 01605, Tel: (508) 831-6839, jmcoburn@wpi.edu.

for neuroblastoma is GD2.[3] GD2 is a ganglioside expressed by both neuroblastoma and melanoma. Expression in non-cancerous tissues is restricted to peripheral sensory neurons and melanocytes, making it a promising therapeutic target.[4,5] There is only one approved GD2 targeting therapeutic in the United States, a chimeric antibody, ch14.18, or DNX, approved for the treatment of high-risk neuroblastoma and administered in combination with IL-2 and GM-CSF.[3,6] Structurally, ch14.18 is a chimeric monoclonal antibody containing an Fc portion of a human IgG1 immunoglobulin fused with the Fab portion of a murine 14.18 monoclonal antibody.[7]

Clinically, DNX has been approved for the treatment of neuroblastoma in combination with IL-2 and GM-CSF.[4,8–10] In a Phase III clinical trial, Yu et al. demonstrated that DNX in combination with GM-CSF and IL-2 was superior to standard therapy in terms of event-free survival rate.[3] The level of GD2 expression within tumors is known to be variable and low levels of GD2 expression have been correlated to higher levels of relapse after receiving immunotherapy.[11] *In vitro* cell lines with differing levels of GD2 have shown differential levels of binding of therapeutics and response to therapeutics.[11]

DNX is delivered via IV infusion at an amount of 17.5 mg/m$^2$/day, over the course of 10 to 20 hours for 4 consecutive days for up to 5 cycles.[12] Due to the large size of antibodies, successful infiltration of the antibody into the tumor bed is difficult.[3,13,14] Additionally, DNX exhibits off-target effects associated with systemic delivery. These off-target effects are primarily due to DNX binding to GD2 expressed on peripheral nerves, resulting in significant pain, capillary leak, and hypersensitivity.[3] In clinical trials, pain has been noted as the most common side effect necessitating pre-dosing with opioids, and in some cases limiting the dosing of ch14.18 administered.[13,15]

One method to potentially increase the concentration of therapeutic reaching the tumor site, while reducing the frequency (DNX is administered for 4 days/cycle, for up to 5 cycles) and severity of side effects is the use of a sustained release local delivery system.[12,16,17] Methods of achieving local delivery of antibodies include the use of microneedle patches, injection of microparticles or hydrogels into a tumor bed, and release from solid matrices.[18–20] There is currently only one clinically available mode of local delivery for oncology therapeutics, Gliadel®.[21] Gliadel® is a biodegradable polymer wafer containing the chemotherapeutic carmustine. The wafer is implanted adjacent to the tumor bed, and sustained release of the therapeutic is achieved utilizing diffusion and polymer degradation.[21]

Silk fibroin derived from the *Bombyx mori* silkworm is a promising biomaterial for therapeutic delivery platforms due to its structure, stability, and minimal immune response *in vivo*.[22–26] It can be processed into many different formats including films, gels, fibers, and lyophilized foams.[22] As a drug delivery platform, silk fibroin has been studied for the sustained release of chemotherapeutic agents for neuroblastoma treatment.[27–29] Previous work with lyophilized silk hydrogel has shown promise in achieving sustained release of monoclonal antibodies.[30] Lyophilized silk fibroin has also been shown to have a stabilizing effect on enzymes and other macromolecules, which is expected to extend to antibodies.[30]

Previous work has shown the effectiveness of delivering DNX from lyophilized silk fibroin foams *in vivo*.[31] Intra-tumoral delivery of DNX-loaded silk fibroin foams resulted in decreased tumor growth rate in an *in vivo* orthotopic model of neuroblastoma.[31] In the work reported here, we aimed to identify the impact of different silk foam formulations on sustained release of DNX. This was evaluated by changing silk molecular weight, concentration, and crystallinity. An *in vitro* assay to determine bioactivity through CDC was developed. Using this assay, the impact of cellular GD2 expression level on CDC induction by DNX was evaluated. Finally, the bioactivity of the released DNX was confirmed. This work proposes a novel usage of a silk fibroin release system to deliver DNX that induces cytotoxicity in GD2-positive NB cell lines.

## Materials and methods

### Anti-GD2 Antibody

The mouse-human chimeric anti-GD2 antibody, DNX, was provided by United Therapeutics (Silver Spring, MD).

### Silk fibroin extraction

Silk fibroin from *Bombyx mori* silkworm cocoons (Tajima Shoji Co Yokohama, Japan), kindly provided by Dr. David L. Kaplan at Tufts University, was extracted as previously described.[22] Briefly, 5 g of cocoons were cut into approximately 1 cm × 1 cm pieces and boiled in 0.02 M $Na_2CO_3$ for 30 min (30 mE; minutes extracted), 60 min (60 mE), or 120 min (120 mE) to extract the sericin, and dried overnight. The dried silk fibroin fibers were then dissolved in 9.3 M LiBr at 60°C for 3 h. The dissolved silk fibroin was dialyzed in 3,500 MWCO dialysis tubing (Fisher Scientific, Hampton, NH) against ultrapure water (Milli-Q® water system Burlington, MA) for 2 d with a minimum of 6 water changes. The aqueous silk fibroin (referred to as silk from here on) solution was stored at 4°C for future use.

### Silk foam fabrication

Silk, concentrated DNX, and glycerol were mixed to yield final concentrations of 10% (w/v) silk, 13.33 mg/mL of DNX (1 mg/foam unless otherwise specified), and a glycerol mass ratio of 25% (w/w silk). For samples fabricated for Fourier transform infrared (FTIR) spectroscopy, DNX solution, was replaced with buffer (20 mM histidine, 0.05% polysorbate 20, 150 mM sodium chloride, pH 6.8) or water (no salt condition), and glycerol was replaced with water. Samples were fabricated in 6 mm diameter cylindrical molds using 75 μL of the solution. The samples were frozen at −20°C overnight, −80°C for at least of 30 min and lyophilized. To render the materials insoluble and vary the crystalline structure of the silk, the lyophilized samples were water vapor annealed at room temperature in the molds and dried at 37°C for 1 h.

### DNX release

Antibody or buffer-only (control) loaded silk foams were placed in 1.7 mL protein low-bind tubes (VWR, Radnor, PA) in a volume of 1.2 mL of phosphate buffered saline (PBS, pH 7.4; VWR, Radnor, PA) at 37°C. At varying time points, 1 mL of PBS was removed and

replaced with fresh PBS. Protein release over the first 24 h was measured via the UV absorbance at 280 nm (Nanodrop 2000, ThermoFisher, Waltham, MA). After 24 hours, the protein release was determined using an enzyme-linked immunosorbent assay. Briefly, release samples were incubated in 96-well tissue culture treated plates (Greiner Bio-One, Kemsmünster, Austria) for 1 h at 37°C. The plates were washed with PBS containing 0.05% Tween-20. Horseradish peroxidase-conjugated goat anti-human IgG Fc (Jackson Labs, Bar Harbor, ME) was added to each well at 40 ng/well in 4.5% (w/v) non-fat milk and 0.05% (v/v) Tween-20 and incubated at 37°C for 30 min. The plates were washed with PBS containing 0.05% Tween-20 and 50 μL of 3,3',5,5'-tetramethylbenzidine substrate (BioFX, VWR, Radnor, PA) was added to the plate. After 15 min, 50 μL of 2 N sulfuric acid was added to stop the reaction. The absorbance was read at 450 nm on a SpectraMax® 250 microplate reader (Molecular Devices, San Jose, CA). A standard curve of DNX was used to convert the absorbance values to drug concentration. The drug release amount over each time point interval was calculated as:

$$Calculated\ Mass\ (t) = C(t) * V - C(t_p) * V_{co} \quad (1)$$

where C(t) is the concentration calculated at time point, t; V is the total volume of the PBS (1.2 mL); $C(t_p)$ is the concentration calculated at the prior time point; $V_{co}$ is the total carry over volume (0.2 mL). This calculation accounts for the DNX mass in the calculated drug concentration as result of carry over volume from PBS remaining at the prior sampling time point. To generate cumulative mass release curves, the cumulative mass at each time point was calculated as:

$$Cumulative\ Mass\ Release(t) = \sum_1^n Calculated\ Mass_n(t) \quad (2)$$

where, n is the time points sampled. To calculation the cumulative percent release, the following equation was used:

$$Cumulative\ Percent\ Release(t) = \frac{Cumulative\ Mass\ Release(t)}{Initial\ Mass\ of\ DNX\ loaded} * 100 \quad (3)$$

## Fourier transform infrared spectroscopy (FTIR)

FTIR spectroscopy was performed with a Bruker Optics Vertex70® (Billerica, MA) equipped with a Specac Golden Gate ATR Crystal (Fort Washington, PA). Samples were removed from the cylindrical mold and pressed into flat wafers using a force of 0.5 N (Pike CrushIR pellet press, Fitchburg, WI). For each measurement, 128 scans of 4 $cm^{-1}$ resolution were taken in adsorption mode. The amide-I region of the FTIR spectra between 1585 $cm^{-1}$ and 1710 $cm^{-1}$ was visually evaluated for changes in the silk protein secondary structure. Peaks centered around 1640 $cm^{-1}$ and 1620 $cm^{-1}$ represent the random coil (RC) and β-sheet (β) confirmation, respectively. These peaks are indicators of the relative crystallinity of the silk foams. The appearance of a peak centered around the 1620 $cm^{-1}$ position indicates a higher crystalline material as compared to a peak centered around the 1640 $cm^{-1}$ position, which indicates an more amorphous structure.

### Scanning electron microscopy (SEM)

The morphology of silk foams fabricated with different formulations was evaluated. Silk foams were hydrated, cut to expose the cross section, and allowed to dry overnight. The dry samples were sputter coated with gold (25 mA, 60 seconds) and imaged with a field emission scanning electron microscope using a 3-kV electron beam (JEOL 7000F, JEOL).

### Cell culturing

KELLY neuroblastoma cells (Millipore Sigma, St. Louis, MO) were maintained in Roswell Park Memorial Institute 1640 (RPMI) medium supplemented with 10% v/v fetal bovine serum, 100 U/mL penicillin, 100 μg/mL streptomycin, and 2mM L-glutamine (Fisher Scientific, Hampton, NH) at 37 °C at 5% $CO_2$ in a humidified environment. SK-N-AS neuroblastoma cells (ATCC, Manassas, VA) were maintained in Dulbecco's Modified Eagle Media supplemented with 10% v/v fetal bovine serum, 100 U/mL penicillin, 100 μg/mL streptomycin, 2mM L-glutamine, and 0.1 mM NEAA (Fisher Scientific, Hampton, NH) at 37°C at 5% $CO_2$ in a humidified environment. Cells were passaged using 0.25% trypsin-EDTA at 70–80% confluence.

### Fluorescence-activated cell sorting (FACS)

Fluorescence-activated cell sorting was performed at the University of Massachusetts Medical Center (Worcester, MA) using an Aria II cell sorter (BD Biosciences, Franklin Lakes, NJ) as previously described.[31] Briefly, KELLY cells were made into a single cell suspension and washed twice with PBS. Anti-GD2 was added at a concentration of 1 μg/$10^6$ cells in a volume of 100 μL/$10^6$ cells and incubated for one hour at 4°C. Cells were washed with PBS and incubated with Alexa Fluor® 488-conjugated goat anti-human IgG secondary antibody (Jackson Laboratories, Bar Harbor, ME) at 1:500 dilution for 40 min at 4°C. Cells were then resuspended in phenol red free media and stained with 7AAD (TONBO Biosciences, San Diego, CA) just prior to sorting at a concentration of 3 μL/mL. The KELLY cells that expressed the highest GD2 (top 12%) and the lowest GD2 (bottom 12%) were collected.

### Flow cytometry

KELLY and SK-N-AS cells were made into a single cell suspension and washed twice with PBS. Cells were incubated with DNX at 1 μg/1×$10^6$ cells in a volume of 100 μL for 1 h at 4°C. Cells were then washed in PBS supplemented with 1% FBS and 0.02% sodium azide at a concentration of 1×$10^6$ cells/mL. Cells were incubated with secondary antibody (Alexa Fluor ®488-conjugated goat anti-human, Jackson Laboratories, Bar Harbor, ME) at a 1:1,000 dilution in PBS at 1×$10^6$ cells in 100 μL for 40 min at 4°C. Cells were then washed twice with PBS, fixed for 10 min with 4% (w/v) paraformaldehyde, and washed twice with PBS. Cells were resuspended at 1×$10^6$ cells in 100 μL. Flow cytometry was performed on an Accuri 6 Flow cytometer (BD, Biosciences, San Jose, CA). Analysis was performed using FlowJo® software with a minimum of 5,000 events captured for each sample.

### Complement-dependent cytotoxicity (CDC) assay

A customized CDC assay was developed to determine the bioactivity of DNX. KELLY neuroblastoma cells were passaged and made into a single cell suspension and stained in 10 μM Calcein (Thermo Fisher, Waltham, MA) at a concentration of $1\times10^6$ cells/mL for 30 min at 37°C. To determine the optimal cell number to differentiate viability from non-viable cells, Calcein-stained and non-stained KELLY neuroblastoma cells were separated into aliquots of $1\times10^5$, $5\times10^4$, $2.5\times10^4$, and $1.25\times10^4$ cells in 100 μL of medium. Then 20 μL of 2% (v/v) Triton X-100 was added to each cell aliquot for complete cell lysis. The cells were incubated at room temperature, protected from light for 2 h. After 2 h, the lysed suspension was centrifuged, and the fluorescence level of the suspension was quantified. For all further experiments, $5 \times 10^4$ cells were used. To determine the toxicity of human complement serum (denoted as complement serum from hereon), Calcein-stained KELLY cells at $5\times10^4$ in 70 μL of medium were treated with 30 μL of complement serum (Innovative Research Inc., Novi, MI) or PBS giving a final concentration (v/v) of 30%, 25%, 20%, and 10%. The cells were incubated at room temperature, protected from light for 2 h. After 2 h, the cell suspension was centrifuged, and the fluorescence of the supernatant was quantified and compared to a dead cell control lysed with 0.3% Triton X-100. For CDC experiments, Calcein-stained cells (KELLY and SK-N-AS) at $5\times10^4$ in 80 μL of medium were treated with 20 μL of DNX solution or release product for 20 min at room temperature. Complement serum or PBS (control) at a final concentration 10% (v/v) was added to the solution and the cells were incubated at room temperature, protected from light for 2 h. After 2 h, the cell suspension was centrifuged, and the fluorescence of the supernatant was quantified. Fluorescence was quantified using an excitation filter of 485 nm and an emissions filter of 535 nm (Perkin Elmer Victor$^3$ Multilabel Counter, Waltham, MA). Additional experiments were performed to confirm that silk did not interfered with the CDC assay. Two forms of silk were investigated – soluble silk doped into the medium (final 420 μg/mL 60 mE silk) and silk potential leaching from the silk foams formulated without loaded DNX (from the PBS supernatant of the 2 h release time point non-DNX loaded silk foam).

### Statistical analysis

All data are presented as mean ± standard deviation from one experiment with three independent samples, except for FTIR analysis, which is presented as a representative sample from each group. Statistical significance was determined by a Student's *t*-test or one-way ANOVA test and Tukey honestly significant difference test using GraphPad Prism (Version 5.01, San Diego, CA).

## Results

### Fabrication of silk fibroin foam for sustained release of anti-GD2

In order to fabricate a sustained release system for DNX, silk foams containing DNX or buffer-only (control) were fabricated via lyophilization as previously described.[31] The silk foams serve to stabilize antibodies and to control antibody release through entrapment and diffusion.[30,32–34] We first evaluated the impact of silk molecular weight and silk concentration on DNX release (Supplementary Figure 1A, 1B). These initial experiments

were carried out for approximately one week to identify conditions for extended release evaluation. Silk at different molecular weights was varied based on extraction times of 30 min (30 mE), 60 min (60 mE), and 120 min (120 mE).[35] The two low molecular weight silk foam formulations, 60 mE and 120 mE at 3.6% (w/v), exhibited a high burst release (76% and 84% in the first 24 h, respectively) with limited sustained release over time (less than 0.5%/day). No difference in burst or sustained release between 60 mE and 120 mE silk foams was observed. Silk foams fabricated at the highest molecular weight (30 mE) and 10% (w/v) exhibited the lowest burst release of 25% in the first 24 h, and a longer sustained release of DNX approximately 2%/day for days 1–5, 0.5%/day for days 5–8 (Figure S1A). The impact of 30 mE silk concentration was compared at 10% and 6% (w/v) (Figure S1B). A similar release profile to the 60 mE and 120 mE silk foams was observed with the 6% silk, with the majority of the DNX released in the first 24 h (94%) with limited sustained release. The 10%, 30 mE silk formulation exhibited a lower burst release than the other formulations. Based on these data, the 10%, 30 mE silk foam formulation exhibited the lowest burst release and sustained release over time and was the formulation for continued characterization.

### Influence of water vapor annealing on silk foam crystallinity and DNX release

To control molecular entrapment of DNX in silk foams, we investigated water vapor annealing times to control silk crystallinity. Exposing silk materials, devoid of other small molecules or macromolecules, to water vapor results in absorption of water effectively reducing the glass transition temperature allowing for molecular reorganization and transitioning from an amorphous structure to a crystalline structure.. When the glass transition temperature drops below the external temperature the silk molecules become mobile and rearrangement into an enrich β-sheet secondary structure. This increase in the β-sheet secondary structure results in insoluble materials. Silk foams composed of 10% (w/v) 30 mE silk loaded with 1 mg of DNX were evaluated. For the pilot release experiments, water vapor annealing lengths of 4, 8, and 24 h were tested. No difference in burst or sustained release were observed based on water vapor annealing (Figure 1). All foams exhibited a similar burst release 11.3 ± 2.4%, 11.6 ± 0.9%, and 14.0 ± 3.1% in the first 24 h for the 4, 8, and 24 h annealing conditions, respectively. The sustained release was also similar with release rates of 0.5 ± 0.26%/day, 0.40 ± 0.28%/day, 0.55 ± 0.16%/day for days 1–7, and 0.02 ± 0.03%/day, 0.01 ± 0.008%/day, and 0.04 ± 0.05%/day for days 7–31 for the 4, 8, and 24 h annealing conditions, respectively.

To examine the influence of water-vapor annealing on crystallinity of the lyophilized silk foams, FTIR spectroscopy was used to analyze crystallinity. Silk foams fabricated containing buffer without DNX were exposed to water vapor for 0.5 h, 1 h, 2 h, 4 h, 8 h, or 24 h. Changes in crystallinity can be noted by a shift from random coil (1631–1655 $cm^{-1}$) to β-sheet structure (1615–1630 $cm^{-1}$).[36–38] No difference in β-sheet content was observed across all water vapor exposure times (Figure 2A). Since the as-lyophilized foams exhibited unexpected crystallinity, formulations were evaluated with the buffer replaced with water and the glycerol replaced with water in all possible combinations (Figure 2B, 2C). Samples formulated with water and glycerol exhibited a shift from a predominantly random coil to β-sheet structure after 30 min exposure to water vapor and an increase in β-sheet

structure with increased exposure time. Samples formulated with water and no glycerol showed similar shifts, though to a lesser extent, possibly due to the hygroscopic nature of glycerol increasing silk hydration and allowing for increasing molecular rearrangement. We also performed SEM on silk foams to observe the microstructure. All silk foam formulations showed similar porous microstructure (Figure 2D–F). These data suggest that the presence of salt within the buffer induced the β-sheet conformation of silk limiting the impact of water vapor annealing on crystallinity and DNX release providing an avenue for further investigation; an important observation when utilizing the water vapor anneal process for formulating sustained release silk materials.

## Release of DNX is reproducible across independent experiments

In order to evaluate reproducibility of DNX, three independent release experiments were carried out. The release profile of 10% (w/v) 30 mE silk foams loaded with 1 mg of DNX were evaluated to determine reproducibility (Figure 3A and B). The foams exhibited an average burst release of 15.8 ± 1.2% in the first 24 h and a sustained release of 0.6 ± 0.4%/day for days 1–7, 0.3 ± 0.1%/day for days 7–17, and 0.07 ± 0.03%/day for the remainder of the experiment. No statistical differences were observed at any time point between repeats of the release experiments.

## Development of a complement dependent cytotoxicity (CDC) assay to evaluate DNX activity

Previously, i*n vitro* complement dependent cytotoxicity (CDC) has been used as to assess cellular responses to GD2 antibodies.[15,31,39,40] One method of evaluation is a Calcein release assay, where live cells are stained with Calcein-AM, and complement induced cell lysis causes the release of Calcein.[41] In this work, we identified optimal parameters to perform the CDC assay with DNX using the KELLY neuroblastoma cell line (Figure 4). First, we determined a cell number (ultimately a cell concentration) that exhibited maximum difference between viable cells (untreated) and completely lysed cells (Triton X-100 treatment) (Figure 4A). A cell number of 50,000 cells in a volume of 100 μL of medium was selected. This cell density allowed for clear differences between viable and non-viable cells without saturating the fluorescence detector (as observed with the 100,000-cell condition). The fluorescence signal was confirmed to be Calcein-only as the 100,000-cell condition without Calcein did not exhibit detectable fluorescence. Next, we identified to maximum concentration of complement serum that did not induce toxicity. Concentrations greater than 10% complement serum induced a statistical increase in cell death as evidenced by the increased fluorescence signal (Figure 4B); all subsequent CDC induction by DNX experiments were performed with 10% complement serum. After determining the cell number and complement serum concentration, cells were treated with DNX and assayed for CDC. No significant toxicity was induced by DNX without complement serum (Figure 4C). With complement serum, CDC induction by DNX concentrations ranging from 500 μg/mL to 0.1 μg/mL (Figure 4C) resulted in a dose-dependent relationship that followed a 4-parameter logarithmic fit with an $R^2$ value of 0.98.

To confirm that the presence or potential presence of silk would not interfere with the CDC assay, cells were treated with varying forms of silk with or without 100 μg/mL DNX. Both

the soluble silk and the silk that potentially leached out of the silk foams at the 2 h time point did not alter the CDC induction by DNX as evidenced by no statistical differences between the two silk conditions containing 100 μg/mL DNX and the 100 μg/mL DNX-only group (Figure 4D). Additionally, soluble silk and the silk that potentially leached out of the silk foams did not induce cell death on their own as evidenced by no statistical differences between the two silk conditions and the untreated cells (Figure 4D).

### Impact of GD2 expression level on CDC using flow sorted KELLY neuroblastoma cells

To determine the impact of GD2 expression level on CDC induction by DNX on KELLY neuroblastoma cells, a CDC assay was performed on KELLY neuroblastoma cells with different expression levels of GD2. KELLY neuroblastoma cells were sorted for GD2 expression level using FACS into cell populations that were positive for GD2 but exhibited different expression levels, labeled as low and high based on the range from unsorted KELLY cells.[31] Confirmation of the retention of low and high GD2 expression level was performed through flow cytometry as cells had undergone approximately 5 passages (Figure 5A). KELLY cells sorted for high GD2 expression level had a median fluorescence of 446,000 and sorted for low GD2 expression level had a median fluorescence of 91,560 while unsorted cells had a median fluorescence of 294,911 (Figure 5A). DNX-treated KELLY cells sorted for high GD2 expression exhibited the highest amount of cell death, with a maximum cell death of 75.9 ± 2.3% achieved when treated with a 500 μg/mL of free DNX (Figure 5B). Comparatively, KELLY cells not sorted for GD2 level (parent cell population) or low GD2 expressing exhibited cell death at 52.0 ± 7.5% 24.4 ± 3.4% when treated with a 500 μg/mL of free DNX, respectively (Figure 5B). At a DNX concentration of 1 μg/mL there was 6.3 ± 0.9%, 33.2 ± 2.4%, and 52.8 ± 0.9% for the low, unsorted and high expressing GD2 cells, respectively.

### Response to DNX treatment as a function of GD2 expression level is conserved when comparing different cell lines

To determine the impact of GD2 expression level on CDC, a neuroblastoma cell line, SK-N-AS, known to express lower GD2 levels as compared to the KELLY cell line was evaluated.[42,43] First, the GD2 expression of the SK-N-AS neuroblastoma cells was compared to KELLY neuroblastoma cells. SK-N-AS cells had a median fluorescence of 66,971 and KELLY cells had a median fluorescence of 249,674, indicating that the entire SK-N-AS cell population has a lower GD2 expression level (Figure 5C). Next, we evaluated DNX-induced CDC on each cell line with varying concentrations of DNX. The results demonstrated significantly less cell death induced by free-DNX on SK-N-AS cells at concentrations above 1 μg/mL as compared to KELLY cells. At the highest free-DNX concentration tested, 500 μg/mL, a difference of 40% cell viability was observed (Figure 5D). These data, in combination with the flow sorted cell data, support the idea that differences in GD2 expression level will result in difference response levels to DNX exposure.

### Released DNX exhibits bioactivity *in vitro*

To evaluate the bioactivity of released of DNX, CDC was evaluated using KELLY neuroblastoma cells. Toxicity of the release product was evaluated using two of the

experiments used to determine reproducible release. Different release time points were evaluated, at different dilution factors to ensure concentrations were within the assay range. The highest amount of cell death correlated with the highest concentration of released DNX, occurring within the first hour of release (Figure 6A). Release product from hours 8–24 of the experiment also demonstrated high toxicity (Figure 6B). Toxicity of release product persisted through day 28 of release (Figure 6C, 6D, 6E). At the first release time point tested an average concentration of 13.2 μg/mL of release product was evaluated, resulting in an average toxicity of 74.2%. When compared to a standard curve utilizing 10 μg/mL a similar toxicity of 71.4% was observed. Similarly, release product from day 3 with an average concentration of 1 μg/mL induced 57.5% toxicity, as compared to the standard curve value of 46.7%. At later timepoints such as day 14, release where an average concentration of 9 μg/mL was evaluated and an average toxicity of 55.9% was observed. At the last time point evaluated, day 28 an average concentration of 0.6 μg/mL of release was evaluated with an average cell death of 29.5%. In all cases (both release and the standard curve) the critical value to induce toxicity greater than 10% was 0.1 μg/mL. This suggests that DNX bioactivity is retained throughout the release experiment.

To determine if this toxicity of the released DNX differed based on GD2 expression level, the toxicity of the release product from hours 8–24 was evaluated using KELLY neuroblastoma cells sorted for high and low GD2 expression levels (Figure 7). The release product was significantly less effective in inducing toxicity on cells with a low expression level of GD2 as compared to a high expression level or the non-sorted cells. The release product induced 56.2% ± 6.8% in cells expressing higher levels of GD2 as compared to non-sorted cells (41.8% ± 4.2%) and cells expressing lower levels of GD2 (19.7% ± 1.5%). This suggests that product from our release experiment exhibits toxicity based on GD2 expression level of the cell population.

## Discussion

DNX is a chimeric antibody that has shown clinical promise in the treatment for high-risk neuroblastoma. It targets the GD2 ganglioside that is expressed on neuroblastoma cells with restricted expression on non-cancerous tissue. ADCC and CDC as mechanisms of action for GD2-targetting antibodies have been demonstrated *in vitro*, *in vivo* in mouse models, and clinically.[44–47] However, problems with the therapy remain including large antibody size limiting infiltration into the tumor bed, and extreme pain is a dose limited side effect experienced by most patients. In addition, after therapy approximately one third of patients still relapse and eventually succumb to the disease.[11] Limitations in treatment efficacy provide an opportunity for the development of a platform capable of local sustained drug release.

Delivering high concentrations of DNX to the tumor site is difficult due to its large size and dose limiting side effects in patients.[8,13,14] One method for delivering higher concentrations of therapy to the tumor site, while reducing the potential negative side effects, is local delivery. In previous work, we reported on the impact of locally delivering DNX to mouse orthotopic NB tumors through lyophilized silk foams and showed that the local delivery significantly decreased tumor growth rates.[48] Lyophilized silk foams are advantageous as

they are better equipped for long term storage than aqueous storage, are easy to handle for implantation, and the fabrication takes place in an all aqueous format eliminating and need for harmful solvents.[30,34] In addition, lyophilization of silk hydrogels has been used previously for the release of bioactive antibodies and has been shown to have a stabilizing effect on enzymes which is expected to extend to antibodies[30,49,50]. The use of silk fibroin also allows for the control over many fabrication parameters including molecular weight of silk, silk concentration, and silk crystallinity. These properties can impact the molecular entrapment of the antibody within the silk, allowing for control over the drug release rate.[51]

The engineered silk foams in this work exhibited a burst release of DNX followed by a sustained release over time. The mechanisms of release are primarily through the diffusion through the silk-phase of the silk foams, hydrophobic/hydrophilic interactions, and hydration resistance to the silk foams, as these have previously been demonstrated with lyophilized silk hydrogels.[30] Through modification of the silk molecular weight and concentrations we attempted to control the molecular entrapment and diffusion of DNX. We observed that silk concentration (a higher amount of silk relative to DNX) led to increased molecular entrapment and slower rate of release. Additionally, silk with a higher molecular weight (lower extraction time) slowed DNX release. This was consistent with previous findings that 10% lyophilized silk hydrogels exhibited a lower burst release of monoclonal antibodies than 3% and 6%, likely due to increased entrapment and hydration resistance.[30] The fabricated silk foams composed of 10% 30 mE silk exhibited a low cumulative release relative to those with a lower silk concentration and molecular weight, with only 20–25% of the loaded DNX being released. In comparison, similar studies where monoclonal antibodies were released from lyophilized silk hydrogels, similar antibody release profiles were observed from lyophilized hydrogels containing 9.2% 60 mE extraction silk (fast burst release with only 15% cumulative release).[30] Lyophilized silk hydrogels fabricated with a lower concentration (3.2% silk) were observed to have a noticeably higher amount of release, with the authors identifying hydration resistance, decreased matrix porosity, and increased silk matrix density as the primary drivers.[30,34] Silk has also been shown to degrade *in vivo*.[52] DNX release may be increased *in vivo*, as silk can be degraded by mammalian-derived enzymes present within the tumor microenvironment, further facilitating DNX release.[53]

Exposure to water vapor has been demonstrated to increase silk crystallinity without the use of complex processing or harsh chemicals (typically organic solvents).[37] In these studies, no impact on crystallinity was observed based on exposure to water vapor. We showed that the lack of difference between water vapor annealed and non-water vapor annealed samples crystallinity was due to salt content in the buffer. Salt has been demonstrated to induce β-sheet formation in silk.[54] Upon evaluating buffer-containing and buffer-free silk foams, we confirmed that the lack of changes in the silk crystallinity upon water vapor exposure was due to the buffer, or salts within the buffer. Antibody buffers are typically formulation to stabilize the pH for long-term antibody stability.[55] The presence of additional components such as Tween-20® and L-histidine have been shown to further stabilize antibodies and minimize protein aggregation.[56,57] However, studies have demonstrated that when antibodies are freeze-dried for long term storage, these buffer components may not be necessary to retain stability.[55] Instead, inclusion of sugars such as sucrose or glycerol

can provide stability through the lyophilization process.[55,58] To tune antibody release from silk foams, additional work needs to be performed to remove buffer components while maintaining antibody stability and investigate the impact of varying the silk crystallinity on antibody release.

In this study, we evaluated response of cells sorted via flow cytometry for high and low GD2 expression level, as well as two different neuroblastoma cell lines to DNX driven CDC. Using cells sorted for GD2 expression level from a single cell line we determined that response to CDC induced lysis was dependent on GD2 level. To our knowledge, this is the first study to demonstrate that response to a GD2-targeting antibody is based on the level of GD2 expression, as use of two different cell lines could introduce compounding variables (such as differences in binding site or cell secretions). However, we note that this finding is supported by prior work evaluating CDC and antibody dependent cellular cytotoxicity using *de novo* established NB cell lines cell lines. Though not specifically stated, the work shows that DNX induced CDC is dependent on the GD-2 expression level of the cell line.[59] In addition, comparison of a cell line with known high GD2 expression level to a cell line with known lower GD2 expression level (SK-N-AS) confirmed these results. Previous literature has evaluated DNX induced cytotoxicity against GD2 expressing and non-GD2 expressing cells.[7,59] DNX exhibited no activity against non-GD2 expressing cells. Therefore, the cytotoxicity observed in this work is expected to be through DNX binding to GD2 on the NB cell surface.

There has been limited clinical work examining GD2 expression level in neuroblastoma patients and its impact on therapeutic efficacy and likelihood of regression. Terzic et al. demonstrated that a low percentage of positive GD2 cells before immunotherapy could be linked to clinical relapse of neuroblastoma.[11] This suggests that a portion of the cells could escape the antibody induced cell lysis allowing the tumor to relapse. However, the effect of DNX on GD2 expression level within patients has not been examined. While studies have suggested that patients retain GD2 expression, the GD2 expression level, and whether that level is sufficient for treatment efficacy has yet to be elucidated.

*In vitro* studies have been performed comparing GD2 expression level across different neuroblastoma tumor cell lines as well as among different tumor cell types. Mujoo et al. demonstrated that neuroblastoma and melanoma cell lines have significantly higher reactivity with ch14.18 via an ELISA assay than other tumor cell lines.[10] Additionally, those studies demonstrated that within neuroblastoma tumor cell lines, while most cell lines contained primarily positive cells, different levels of binding were present. These differences may directly correlate with cell responsiveness to ADCC and CDC assays.[10] This was further confirmed by Esser et al. and Terzic et al, who both demonstrated a correlation between GD2 expression level as demonstrated by flow cytometry and ADCC.[11,60] These studies demonstrated that low expressing GD2 tumors can respond to anti-GD2 treatment, but may require a higher concentration to induce cell death.[10,11,60]

A critical factor in the design of an antibody release systems is its ability to release bioactive antibody. In this work, we evaluated the bioactivity of the release product using a CDC assay. Our results demonstrate the retention of DNX bioactivity for 28 days, which extends

beyond the typical DNX treatment cycle of 20 days (5 courses of 4 days).[61] Further, our release results demonstrate efficacy on cells expressing a range of GD2 expression. This could mimic the range of positive, yet heterogeneously distributed expression within and *in vivo* tumor.

## Conclusions

This work demonstrates the development of a delivery system for DNX with bioactive release through 28 days. The DNX release was not altered by water vapor annealing time, a common method used to tune release through altering the silk crystallinity, as the salts present within the formulations due to the antibody buffer altered the crystalline structure of the lyophilized silk foams. In testing this bioactivity of the DNX, this work reports the importance of GD2 expression level as an important factor for DNX induce CDC in an NB cell line sorted for different levels of GD2 expression using FACS and across two different NB cell lines with different GD2 expression levels. Future studies will develop increased control over release through the exclusion of salts or altering the salt composition and types to allow for control over silk foam crystallinity and DNX release.

## Supplementary Material

Refer to Web version on PubMed Central for supplementary material.

## Acknowledgements

This work was supported by the National Institutes of Health grant R01NS094218 (B.C.) and United Therapeutics research grant (B.C. and J.M.C).

## References

1. Maris JM, Hogarty MD, Bagatell R, Cohn SL. Neuroblastoma. The Lancet 2007;369(9579):2106–2120.
2. Sait S, Modak S. Anti-GD2 immunotherapy for neuroblastoma. Expert review of anticancer therapy 2017;17(10):889–904. [PubMed: 28780888]
3. Yu AL, Gilman AL, Ozkaynak MF, London WB, Kreissman SG, Chen HX, Smith M, Anderson B, Villablanca JG, Matthay KK and et al. . Anti-GD2 antibody with GM-CSF, interleukin-2, and isotretinoin for neuroblastoma. The New England journal of medicine 2010;363(14):1324–34. [PubMed: 20879881]
4. Ahmed M, Cheung NKV. Engineering anti-GD2 monoclonal antibodies for cancer immunotherapy. Febs Letters 2014;588(2):288–297. [PubMed: 24295643]
5. Zhang SL, CordonCardo C, Zhang HS, Reuter VE, Adluri S, Hamilton WB, Lloyd KO, Livingston PO. Selection of tumor antigens as targets for immune attack using immunohistochemistry .1. Focus on gangliosides. International Journal of Cancer 1997;73(1):42–49. [PubMed: 9334808]
6. Perez Horta Z, Goldberg JL, Sondel PM. Anti-GD2 mAbs and next-generation mAb-based agents for cancer therapy. Immunotherapy 2016;8(9):1097–117. [PubMed: 27485082]
7. Soman G, Kallarakal AT, Michiel D, Yang X, Saptharish N, Jiang H, Giardina S, Gilly J, Mitra G. Analytical characterization of ch14.18: a mouse-human chimeric disialoganglioside-specific therapeutic antibody. mAbs 2012;4(1):84–100. [PubMed: 22327432]
8. Yu AL, Gilman AL, Ozkaynak MF, London WB, Kreissman SG, Chen HX, Smith M, Anderson B, Villablanca JG, Matthay KK. Anti-GD2 antibody with GM-CSF, interleukin-2, and isotretinoin for neuroblastoma. New England Journal of Medicine 2010;363(14):1324–1334.

9. Handgretinger R, Baader P, Dopfer R, Klingebiel T, Reuland P, Treuner J, Reisfeld RA, Niethammer D. A phase I study of neuroblastoma with the anti-ganglioside GD2 antibody 14.G2a. Cancer immunology, immunotherapy : CII 1992;35(3):199–204. [PubMed: 1638557]
10. Mujoo K, Cheresh DA, Yang HM, Reisfeld RA. Disialoganglioside GD2 on human neuroblastoma cells: target antigen for monoclonal antibody-mediated cytolysis and suppression of tumor growth. Cancer Res 1987;47(4):1098–104. [PubMed: 3100030]
11. Terzic T, Cordeau M, Herblot S, Teira P, Cournoyer S, Beaunoyer M, Peuchmaur M, Duval M, Sartelet H. Expression of Disialoganglioside (GD2) in Neuroblastic Tumors: A Prognostic Value for Patients Treated With Anti-GD2 Immunotherapy. Pediatr Dev Pathol 2018;21(4):355–362. [PubMed: 29067879]
12. Hoy SM. Dinutuximab: A Review in High-Risk Neuroblastoma. Targeted oncology 2016;11(2):247–53. [PubMed: 26891967]
13. Navid F, Santana VM, Barfield RC. Anti-GD2 antibody therapy for GD2-expressing tumors. Current cancer drug targets 2010;10(2):200–9. [PubMed: 20201786]
14. Beckman RA, Weiner LM, Davis HM. Antibody constructs in cancer therapy: protein engineering strategies to improve exposure in solid tumors. Cancer 2007;109(2):170–9. [PubMed: 17154393]
15. Zeng Y, Fest S, Kunert R, Katinger H, Pistoia V, Michon J, Lewis G, Ladenstein R, Lode HN. Anti-neuroblastoma effect of ch14.18 antibody produced in CHO cells is mediated by NK-cells in mice. Molecular Immunology 2005;42(11):1311–1319. [PubMed: 15950727]
16. Milling L, Zhang Y, Irvine DJ. Delivering safer immunotherapies for cancer. Adv Drug Deliv Rev 2017;114:79–101. [PubMed: 28545888]
17. Harris J, Klonoski SC, Chiu B. Clinical Considerations of Focal Drug Delivery in Cancer Treatment. Current drug delivery 2017;14(5):588–596. [PubMed: 28240175]
18. Chandrasekhar S, Iyer LK, Panchal JP, Topp EM, Cannon JB, Ranade VV. Microarrays and microneedle arrays for delivery of peptides, proteins, vaccines and other applications. Expert Opin Drug Deliv 2013;10(8):1155–70. [PubMed: 23662940]
19. Sherwood JK, Dause RB, Saltzman WM. Controlled antibody delivery systems. Biotechnology (N Y) 1992;10(11):1446–9. [PubMed: 1369022]
20. Schweizer D, Serno T, Goepferich A. Controlled release of therapeutic antibody formats. Eur J Pharm Biopharm 2014;88(2):291–309. [PubMed: 25125350]
21. Westphal M, Hilt DC, Bortey E, Delavault P, Olivares R, Warnke PC, Whittle IR, Jääskeläinen J, Ram Z. A phase 3 trial of local chemotherapy with biodegradable carmustine (BCNU) wafers (Gliadel wafers) in patients with primary malignant glioma. Neuro-oncology 2003;5(2):79–88. [PubMed: 12672279]
22. Rockwood DN, Preda RC, Yücel T, Wang X, Lovett ML, Kaplan DL. Materials fabrication from Bombyx mori silk fibroin. Nature protocols 2011;6(10):1612–31. [PubMed: 21959241]
23. Jewell M, Daunch W, Bengtson B, Mortarino E. The development of SERI® Surgical Scaffold, an engineered biological scaffold. Annals of the New York Academy of Sciences 2015;1358:44–55. [PubMed: 26376101]
24. Ma X, Cao C, Zhu H. The biocompatibility of silk fibroin films containing sulfonated silk fibroin. Journal of Biomedical Materials Research, Part B: Applied Biomaterials 2006;78(1):89–96.
25. Meinel L, Hofmann S, Karageorgiou V, Kirker-Head C, McCool J, Gronowicz G, Zichner L, Langer R, Vunjak-Novakovic G, Kaplan DL. The inflammatory responses to silk films in vitro and in vivo. Biomaterials 2005;26(2):147–55. [PubMed: 15207461]
26. Panilaitis B, Altman GH, Chen J, Jin HJ, Karageorgiou V, Kaplan DL. Macrophage responses to silk. Biomaterials 2003;24(18):3079–85. [PubMed: 12895580]
27. Seib FP, Coburn J, Konrad I, Klebanov N, Jones GT, Blackwood B, Charest A, Kaplan DL, Chiu B. Focal therapy of neuroblastoma using silk films to deliver kinase and chemotherapeutic agents in vivo. Acta Biomaterialia 2015;20:32–8. [PubMed: 25861948]
28. Coburn J, Harris J, Zakharov AD, Poirier J, Ikegaki N, Kajdacsy-Balla A, Pilichowska M, Lyubimov AV, Shimada H, Kaplan DL and et al. . Implantable chemotherapy-loaded silk protein materials for neuroblastoma treatment. International journal of cancer 2017;140(3):726–735. [PubMed: 27770551]

29. Chiu B, Coburn J, Pilichowska M, Holcroft C, Seib FP, Charest A, Kaplan DL. Surgery combined with controlled-release doxorubicin silk films as a treatment strategy in an orthotopic neuroblastoma mouse model. British Journal of Cancer 2014;111(4):708–715. [PubMed: 24921912]
30. Guziewicz N, Best A, Perez-Ramirez B, Kaplan DL. Lyophilized silk fibroin hydrogels for the sustained local delivery of therapeutic monoclonal antibodies. Biomaterials 2011;32(10):2642–50. [PubMed: 21216004]
31. Ornell KJ, Taylor Jordan, Zeki Jasmine, Ikegaki Naohiko, Shimada Hiroyuki, Coburn Jeannine M., Chiu Bill. Local delivery of dinutuximab from lyophilized silk fibroin foams for treatment of an orthtopic neuroblastoma models. Cancer Medicine 2020.
32. Yavuz B, Morgan JL, Herrera C, Harrington K, Perez-Ramirez B, LiWang PJ, Kaplan DL. Sustained release silk fibroin discs: Antibody and protein delivery for HIV prevention. J Control Release 2019;301:1–12. [PubMed: 30876951]
33. Zhang L, Herrera C, Coburn J, Olejniczak N, Ziprin P, Kaplan DL, LiWang PJ. Stabilization and Sustained Release of HIV Inhibitors by Encapsulation in Silk Fibroin Disks. ACS Biomaterials Science & Engineering 2017;3(8):1654–1665. [PubMed: 33225060]
34. Guziewicz NA, Massetti AJ, Perez-Ramirez BJ, Kaplan DL. Mechanisms of monoclonal antibody stabilization and release from silk biomaterials. Biomaterials 2013;34(31):7766–75. [PubMed: 23859659]
35. Wray LS, Hu X, Gallego J, Georgakoudi I, Omenetto FG, Schmidt D, Kaplan DL. Effect of processing on silk-based biomaterials: reproducibility and biocompatibility. Journal of Biomedical Materials Research, Part B: Applied Biomaterials 2011;99(1):89–101.
36. Lawrence BD, Omenetto F, Chui K, Kaplan DL. Processing methods to control silk fibroin film biomaterial features. Journal of Materials Science 2008;43(21):6967–6985.
37. Hu X, Shmelev K, Sun L, Gil E-S, Park S-H, Cebe P, Kaplan DL. Regulation of silk material structure by temperature-controlled water vapor annealing. Biomacromolecules 2011;12(5):1686–96. [PubMed: 21425769]
38. Hu X, Kaplan D, Cebe P. Determining Beta-Sheet Crystallinity in Fibrous Proteins by Thermal Analysis and Infrared Spectroscopy. Macromolecules 2006;39(18):6161–6170.
39. Mueller BM, Romerdahl C, Gillies S, Reisfeld R. Enhancement of antibody-dependent cytotoxicity with a chimeric anti-GD2 antibody. The Journal of Immunology 1990;144(4):1382–1386. [PubMed: 2303711]
40. Lin CC, Shen YC, Chuang CK, Liao SK. Analysis of a murine anti-ganglioside GD2 monoclonal antibody expressing both IgG2a and IgG3 isotypes: monoclonality, apoptosis triggering, and activation of cellular cytotoxicity on human melanoma cells. Adv Exp Med Biol 2001;491:419–29. [PubMed: 14533812]
41. Prang N, Preithner S, Brischwein K, Göster P, Wöppel A, Müller J, Steiger C, Peters M, Baeuerle PA, da Silva AJ. Cellular and complement-dependent cytotoxicity of Ep-CAM-specific monoclonal antibody MT201 against breast cancer cell lines. British journal of cancer 2005;92(2):342–9. [PubMed: 15655555]
42. Craddock JA, Lu A, Bear A, Pule M, Brenner MK, Rooney CM, Foster AE. Enhanced tumor trafficking of GD2 chimeric antigen receptor T cells by expression of the chemokine receptor CCR2b. J Immunother 2010;33(8):780–8. [PubMed: 20842059]
43. Acosta S, Lavarino C, Paris R, Garcia I, de Torres C, Rodríguez E, Beleta H, Mora J. Comprehensive characterization of neuroblastoma cell line subtypes reveals bilineage potential similar to neural crest stem cells. BMC Dev Biol 2009;9:12. [PubMed: 19216736]
44. Barry WE, Jackson JR, Asuelime GE, Wu HW, Sun J, Wan Z, Malvar J, Sheard MA, Wang L, Seeger RC and others. Activated Natural Killer Cells in Combination with Anti-GD2 Antibody Dinutuximab Improve Survival of Mice after Surgical Resection of Primary Neuroblastoma. Clin Cancer Res 2018.
45. Tarek N, Le Luduec JB, Gallagher MM, Zheng J, Venstrom JM, Chamberlain E, Modak S, Heller G, Dupont B, Cheung NK and others. Unlicensed NK cells target neuroblastoma following anti-GD2 antibody treatment. J Clin Invest 2012;122(9):3260–70. [PubMed: 22863621]

46. Siebert N, Seidel D, Eger C, Juttner M, Lode HN. Functional bioassays for immune monitoring of high-risk neuroblastoma patients treated with ch14.18/CHO anti-GD2 antibody. PLoS One 2014;9(9):e107692. [PubMed: 25226154]
47. Yu AL, Uttenreuther-Fischer MM, Huang CS, Tsui CC, Gillies SD, Reisfeld RA, Kung FH. Phase I trial of a human-mouse chimeric anti-disialoganglioside monoclonal antibody ch14.18 in patients with refractory neuroblastoma and osteosarcoma. J Clin Oncol 1998;16(6):2169–80. [PubMed: 9626218]
48. Ornell KJ, Taylor JS, Zeki J, Ikegaki N, Shimada H, Coburn JM, Chiu B. Local delivery of dinutuximab from lyophilized silk fibroin foams for treatment of an orthotopic neuroblastoma model. Cancer Medicine 2020;9(8):2891–2903. [PubMed: 32096344]
49. Li AB, Kluge JA, Guziewicz NA, Omenetto FG, Kaplan DL. Silk-based stabilization of biomacromolecules. J Control Release 2015;219:416–30. [PubMed: 26403801]
50. Kluge JA, Li AB, Kahn BT, Michaud DS, Omenetto FG, Kaplan DL. Silk-based blood stabilization for diagnostics. Proc Natl Acad Sci U S A 2016;113(21):5892–7. [PubMed: 27162330]
51. Rnjak-Kovacina J, Wray LS, Burke KA, Torregrosa T, Golinski JM, Huang W, Kaplan DL. Lyophilized Silk Sponges: A Versatile Biomaterial Platform for Soft Tissue Engineering. ACS biomaterials science & engineering 2015;1(4):260–270. [PubMed: 25984573]
52. Wang Y, Rudym DD, Walsh A, Abrahamsen L, Kim HJ, Kim HS, Kirker-Head C, Kaplan DL. In vivo degradation of three-dimensional silk fibroin scaffolds. Biomaterials 2008;29(24–25):3415–28. [PubMed: 18502501]
53. Brown J, Lu CL, Coburn J, Kaplan DL. Impact of silk biomaterial structure on proteolysis. Acta Biomaterialia 2015;11:212–21. [PubMed: 25240984]
54. Kim UJ, Park J, Kim HJ, Wada M, Kaplan DL. Three-dimensional aqueous-derived biomaterial scaffolds from silk fibroin. Biomaterials 2005;26(15):2775–2785. [PubMed: 15585282]
55. Garidel P, Pevestorf B, Bahrenburg S. Stability of buffer-free freeze-dried formulations: A feasibility study of a monoclonal antibody at high protein concentrations. European Journal of Pharmaceutics and Biopharmaceutics 2015;97:125–139. [PubMed: 26455339]
56. Kerwin BA, Heller MC, Levin SH, Randolph TW. Effects of tween 80 and sucrose on acute short-term stability and long-term storage at −20 degrees C of a recombinant hemoglobin. Journal of Pharmaceutical Sciences 1998;87(9):1062–1068. [PubMed: 9724555]
57. Falconer RJ, Chan C, Hughes K, Munro TP. Stabilization of a monoclonal antibody during purification and formulation by addition of basic amino acid excipients. Journal of Chemical Technology and Biotechnology 2011;86(7):942–948.
58. Cleland JL, Lam X, Kendrick B, Yang J, Yang TH, Overcashier D, Brooks D, Hsu C, Carpenter JF. A specific molar ratio of stabilizer to protein is required for storage stability of a lyophilized monoclonal antibody. Journal of Pharmaceutical Sciences 2001;90(3):310–321. [PubMed: 11170024]
59. Siebert N, Seidel D, Eger C, Jüttner M, Lode HN. Functional Bioassays for Immune Monitoring of High-Risk Neuroblastoma Patients Treated with ch14.18/CHO Anti-GD2 Antibody. PLOS ONE 2014;9(9):e107692. [PubMed: 25226154]
60. Esser R, Muller T, Stefes D, Kloess S, Seidel D, Gillies SD, Aperlo-Iffland C, Huston JS, Uherek C, Schonfeld K and others. NK cells engineered to express a GD2 -specific antigen receptor display built-in ADCC-like activity against tumour cells of neuroectodermal origin. J Cell Mol Med 2012;16(3):569–81. [PubMed: 21595822]
61. Bartholomew J, Washington T, Bergeron S, Nielson D, Saggio J, Quirk L. Dinutuximab: A Novel Immunotherapy in the Treatment of Pediatric Patients With High-Risk Neuroblastoma. Journal of Pediatric Oncology Nursing 2017;34(1):5–12. [PubMed: 27456981]

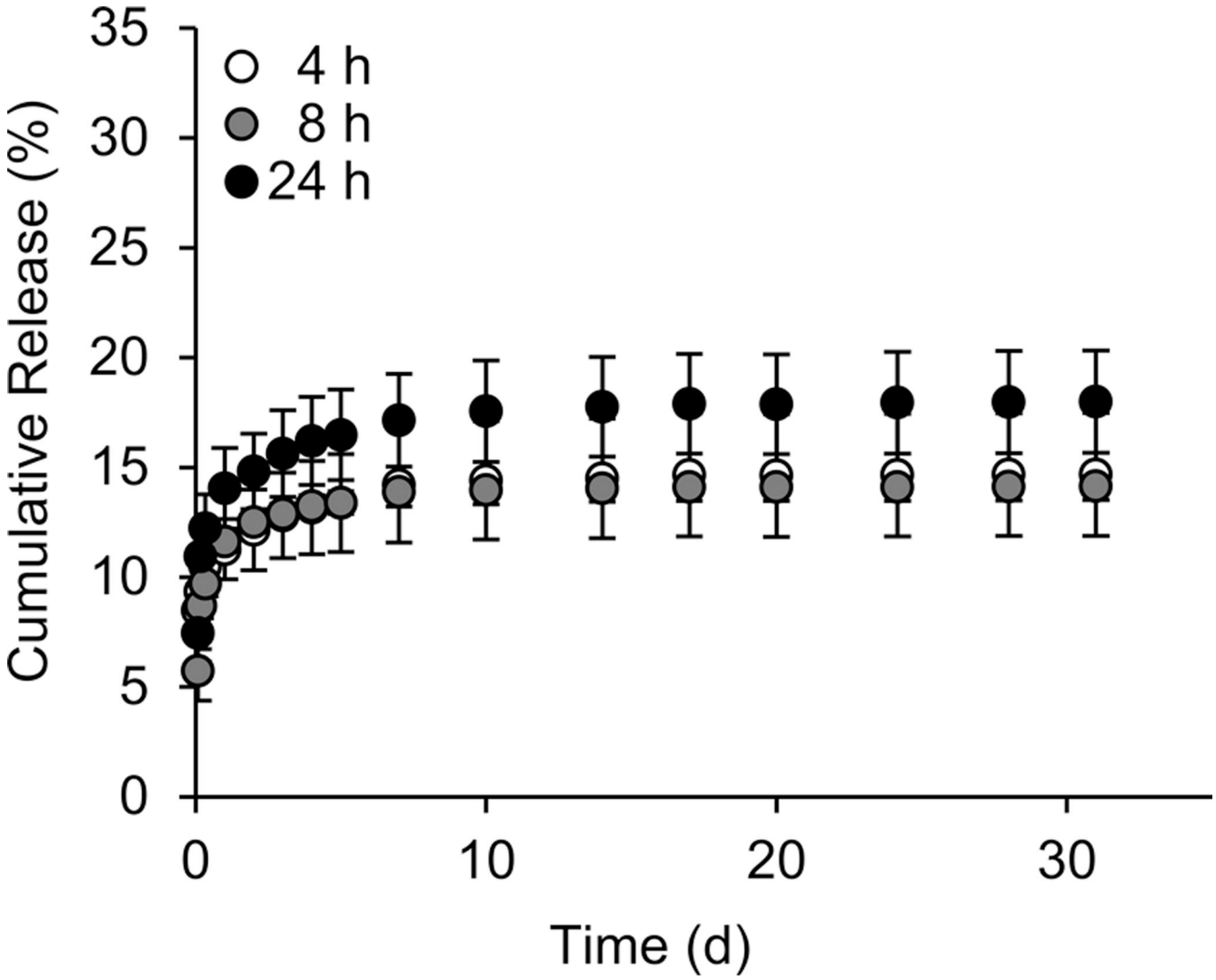


**Figure 1. Impact of water vapor annealing time on DNX release.**

Cumulative release of DNX-loaded silk foams was evaluated. DNX-loaded silk foams were exposed to water vapor for 4 h, 8 h, and 24 h. Data are presented as mean ± standard deviation of three independent samples.

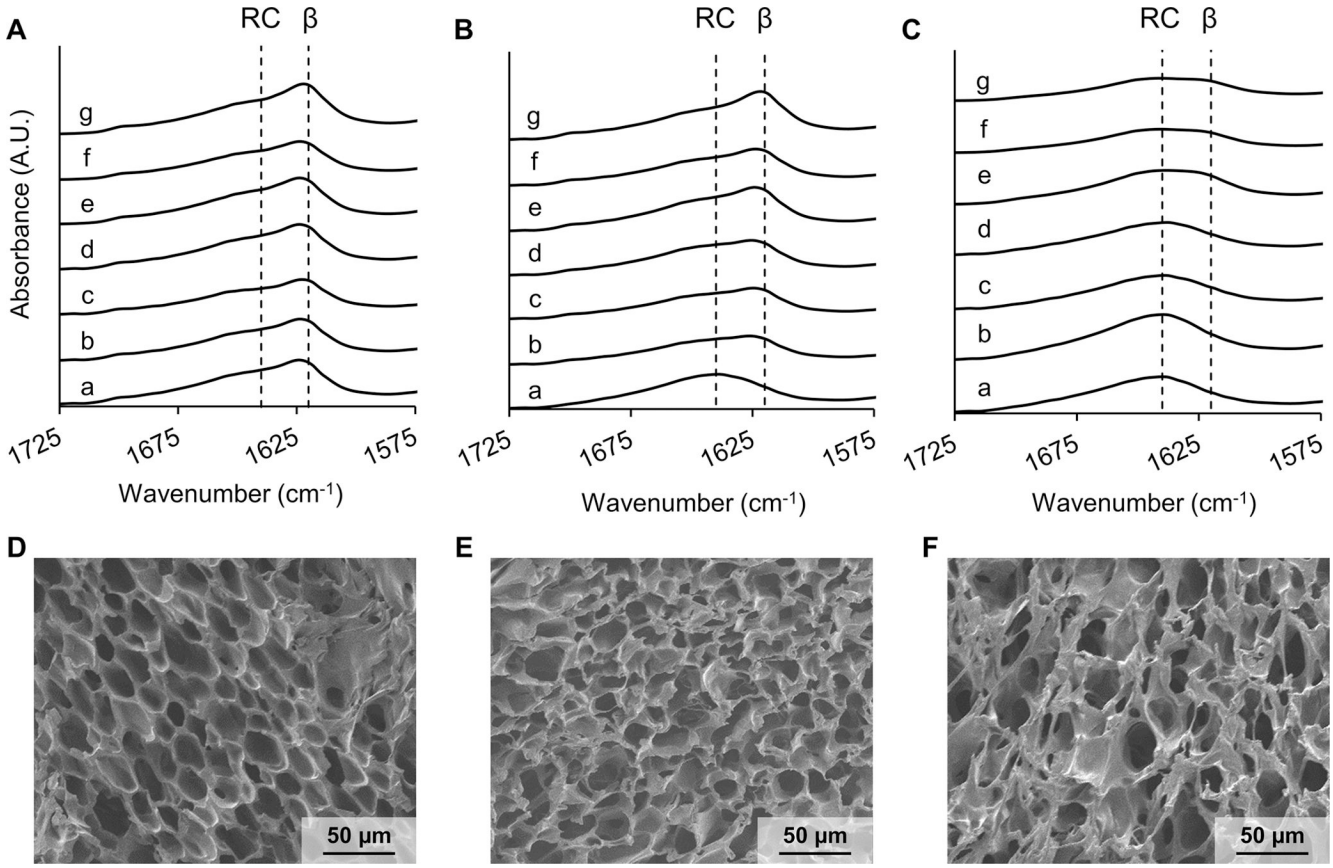


**Figure 2. Impact of DNX buffer components on silk foam secondary structure.**

ATR-FTIR spectrum of 10%, 30-minute extraction silk foams containing (A) buffer and glycerol, (B) water and glycerol, and (C) water only. Each silk foam formulation was either (a) not annealed or annealed for (b) 0.5 h, (c) 1 h, (d) 2 h, (e) 4 h, (f) 8 h, or (g) 24 h. RC represents a random coil peak and B represents a β-sheet peak within the amide I region of the silk. SEM images of the silk foams containing (D) buffer and glycerol, (E) water and glycerol, and (F) water only.

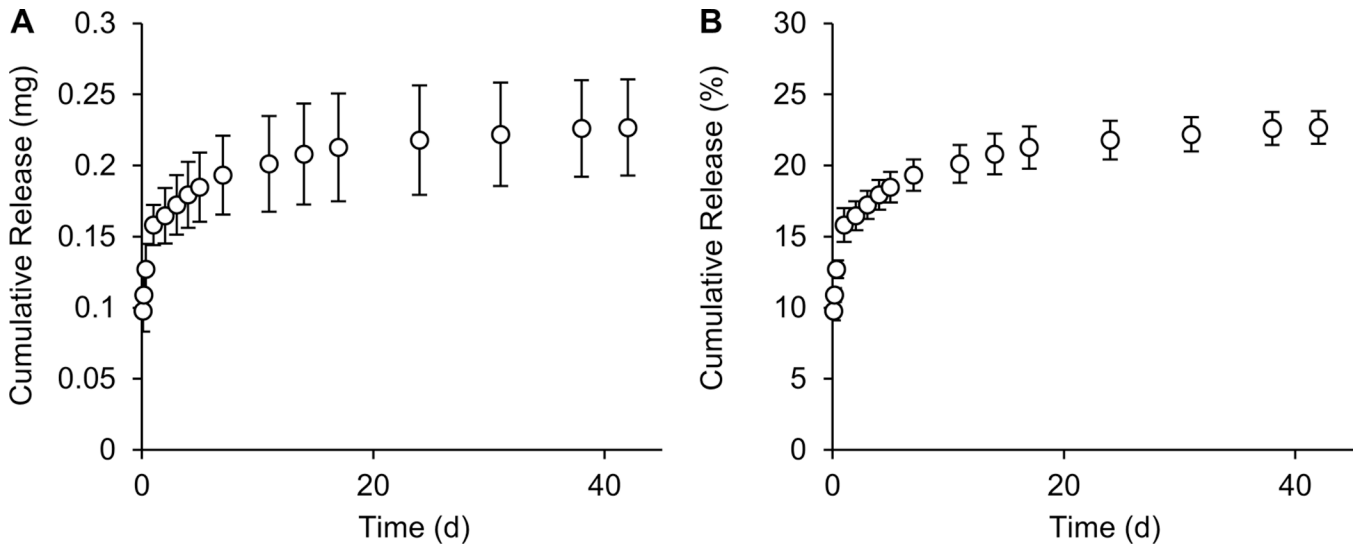


**Figure 3. Cumulative release of DNX from silk foams.**

10%, 30-minute extraction silk foams loaded with 1 mg of DNX and water vapor annealed for 4 hours were evaluated for (A) cumulative mass release and (B) cumulative percent release of DNX. Data are presented as mean ± standard deviation of three independent experiments.

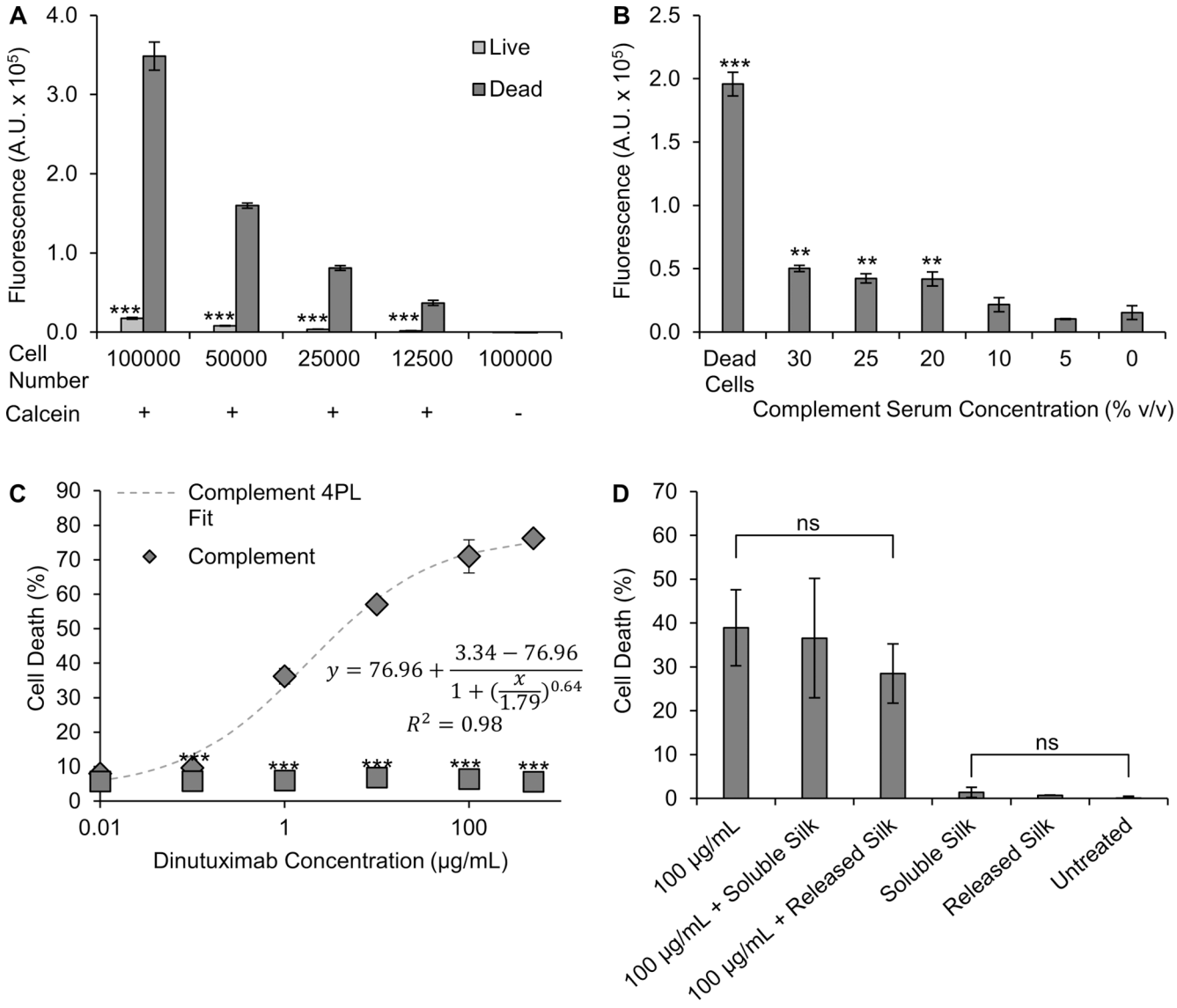


**Figure 4. Determination of CDC assay parameters.**

Identification of (A) number of cells needed for CDC assay, (B) toxicity of complement serum, and (C) toxicity of DNX with and without complement serum. (D) Interference of silk formats with the assay was investigated via soluble silk added to the culture medium (silk) or supernatant from silk foam release experiments (silk release; note these are control samples not loaded with DNX). The presence of silk did not interfere with the assay. Data are presented as mean ± standard deviation of three independent samples. (A) *** $p<0.001$ as compared to dead cells based on a *t*-test. (B) ** $p<0.01$, *** $p<0.001$ when compared to non-complement serum treatment based on one-way ANOVA followed by Tukey's post hoc test. (C) *** $p<0.001$ as compared to DNX-matched concentration with complement serum based on a *t*-test.

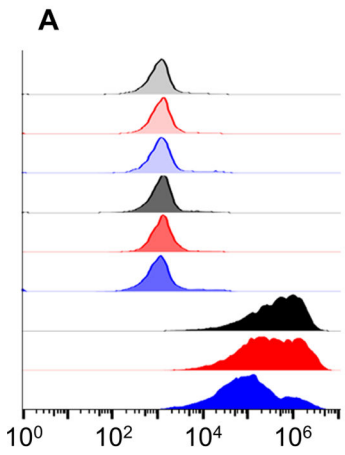


| Subset Name | Median Fluorescence |
|---|---|
| High Blank | 1055 |
| Unsorted Blank | 1168 |
| Low Blank | 1144 |
| High Secondary | 1177 |
| Unsorted Secondary | 1226 |
| Low Secondary | 1046 |
| High | 446,000 |
| Unsorted | 294,911 |
| Low | 91,560 |

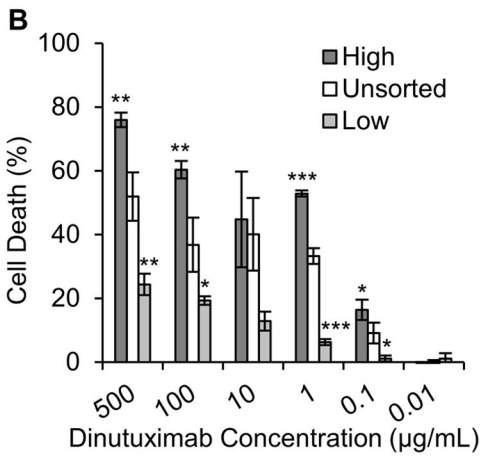


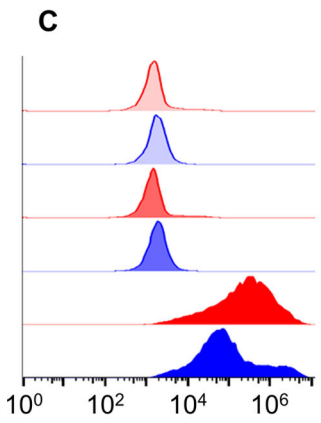


| Subset Name | Median Fluorescence |
|---|---|
| KELLY Blank | 1454 |
| SK-N-AS Blank | 1781 |
| KELLY Secondary | 1396 |
| SK-N-AS Secondary | 1825 |
| KELLY | 249,674 |
| SK-N-AS | 68,345 |

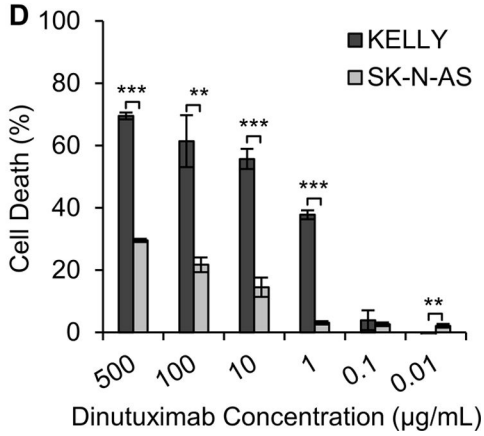


**Figure 5. Impact of GD2 expression on DNX-induced cytotoxicity.**

(A) Flow cytometry analysis of GD2 expression performed in parallel with the CDC assay. (B) CDC of KELLY neuroblastoma cells sorted through fluorescent activated cell sorting for high and low expression of GD2. Cells were exposed to DNX and complement serum. (C) Flow cytometry analysis of GD2 expression of KELLY and SK-N-AS cells performed in parallel with the CDC assay. (D) CDC of KELLY neuroblastoma cells as compared to SKNAS neuroblastoma cells. Data are presented as mean ± standard deviation of three independent samples. (B) *$p < 0.05$, **$p < 0.01$, ***$p < 0.001$ when comparing to unsorted cells based on one-way ANOVA followed by Tukey's post hoc test. (D) *$p < 0.05$, **$p < 0.01$, ***$p < 0.001$ when comparing to SK-N-AS cells based on a *t*-test.

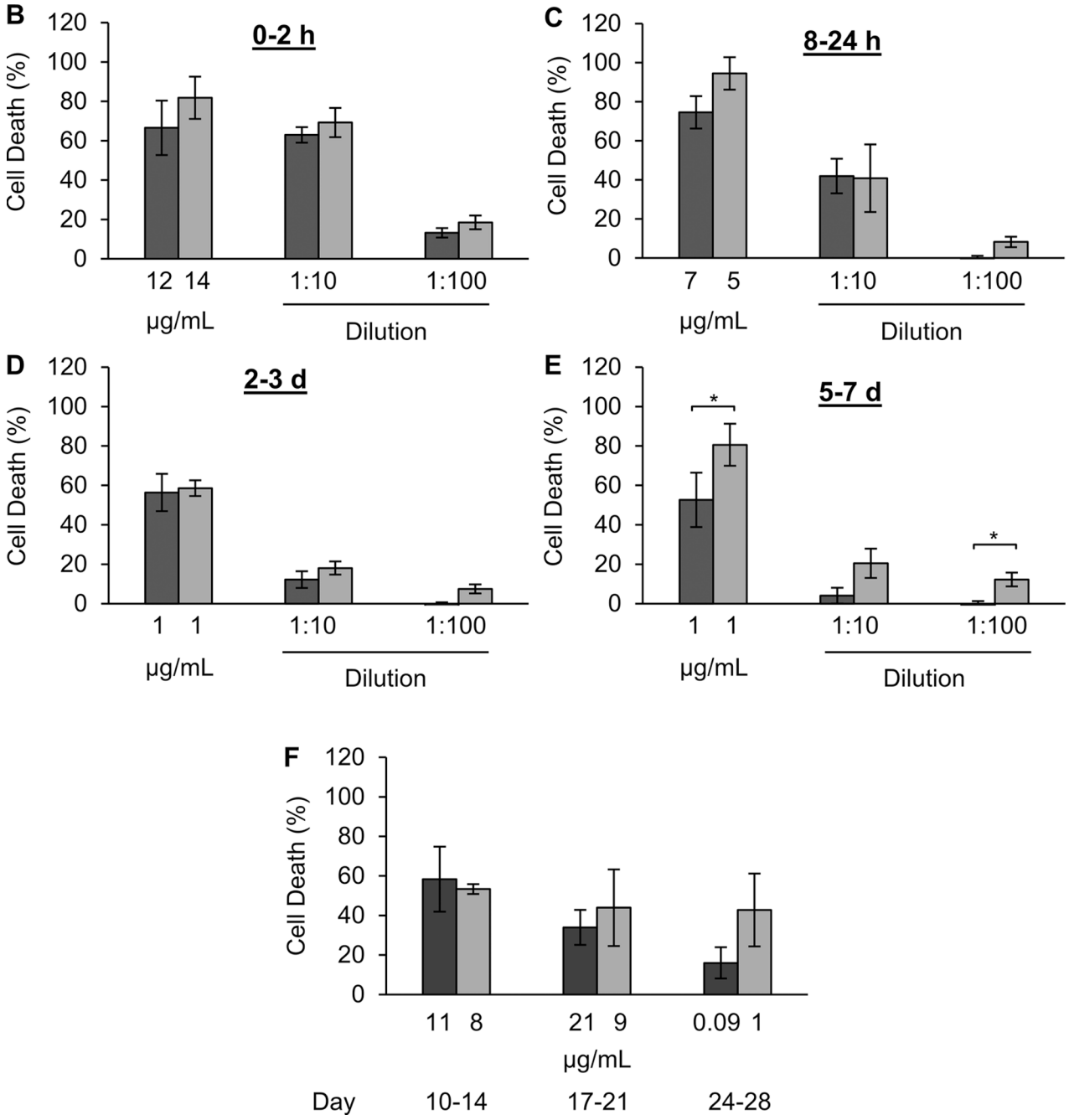


**Figure 6. Effect of release DNX treatment on complement dependent cytotoxicity using unsorted KELLY cells.**

10%, 30-minute extraction silk foams loaded with 1 mg of DNX and water vapor annealed for 4 hours were evaluated. Complement dependent cytotoxicity of DNX release product from (A) hours 0–1, (B) hours 8–24, (C) day 2–3, (D) day 5–7, and (E) to day 28 of release study. Concentration reported are calculated directly from the UV absorbance at 280 nm or enzyme-linked immunosorbent assay and not adjusted for carry over volume to represent the actual DNX concentration within the assay. Data are presented as mean ± standard deviation

of three independent samples. Cytotoxicity data are normalized to complement only control and lysed cell control. *$p < 0.05$ based on a *t*-test.

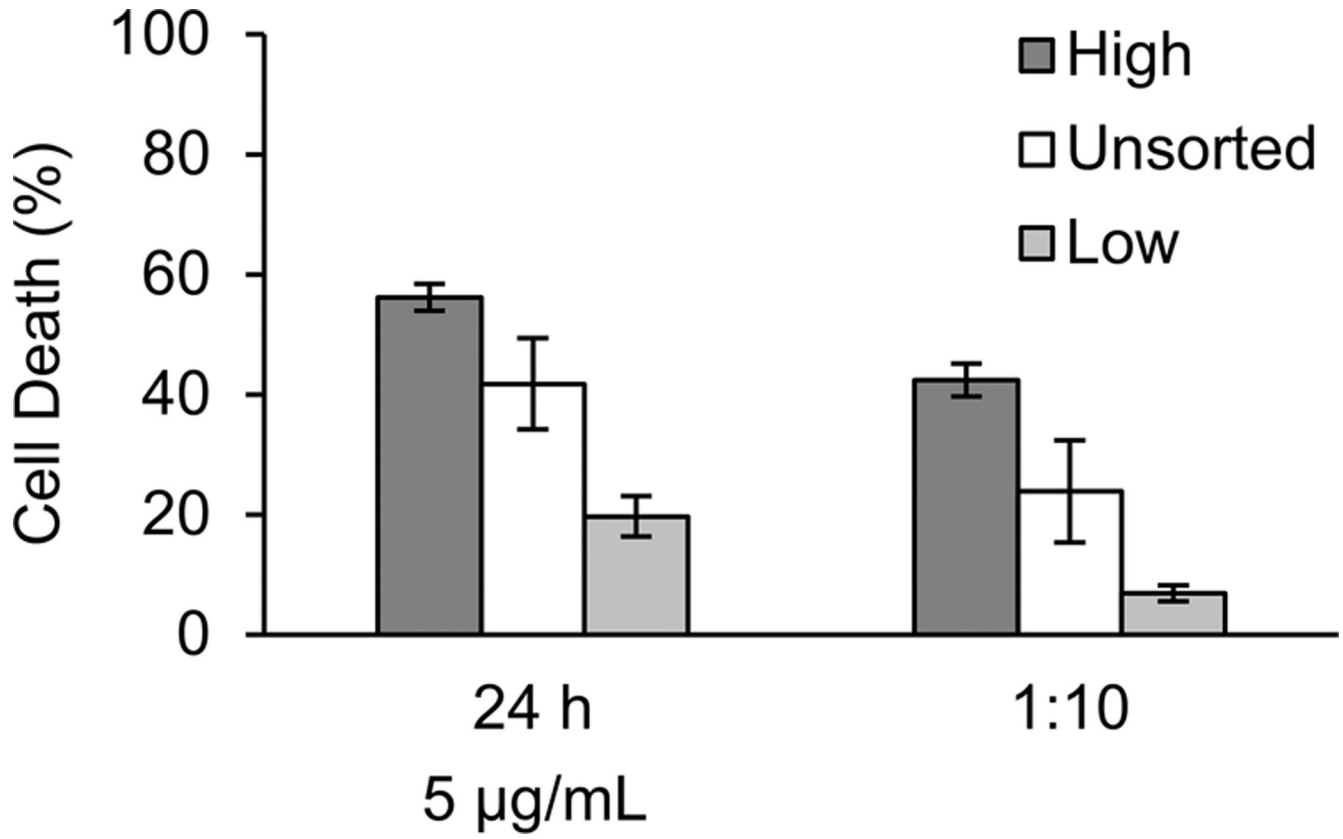


**Figure 7. Effect of release DNX treatment on complement dependent cytotoxicity using KELLY cells with different levels of GD2 expression.**

10%, 30-minute extraction silk foams loaded with 1 mg of DNX and water vapor annealed for 4 hours were evaluated. Complement dependent cytotoxicity assay using KELLY neuroblastoma cells sorted for higher and low GD2 expression, and unsorted was evaluated using release product from hours 8–24. Data are presented two different experiments (dark grey and light grey bars) with mean ± standard deviation of three independent samples.